

Extrasolar planet taxonomy: a new statistical approach

Simone Marchi

*Dipartimento di Astronomia, Università di Padova
vicolo dell'Osservatorio 2, 35122 Padova, Italy*

simone.marchi@unipd.it

ABSTRACT

In this paper we present the guidelines for an extrasolar planet taxonomy. The discovery of an increasing number of extrasolar planets showing a vast variety of *planetary parameters*, like Keplerian orbital elements and *environmental parameters*, like stellar masses, spectral types, metallicity etc., prompts the development of a planetary taxonomy. In this work via principal component analysis followed by hierarchical clustering analysis, we report the definition of five robust groups of planets. We also discuss the physical relevance of such analysis, which may provide a valid basis for disentangling the role of the several physical parameters involved in the processes of planet formation and subsequent evolution. For instance, we were able to divide the hot Jupiters into two main groups on the basis of their stellar masses and metallicities. Moreover, for some groups, we find strong correlations between metallicity, semi-major axis and eccentricity. The implications of these findings are discussed.

Subject headings: planetary systems — planetary systems: formation — planets and satellites: general

1. Introduction

With the discovery of the first extrasolar planet (EP) orbiting a solar-like star (Mayor & Queloz 1995) a new field of astronomical research started. So far, more than 200 extrasolar planets have been discovered. Despite severe observational biases -only partially overcome by the development of more sophisticated techniques and facilities- the most striking fact is the vast variety of EPs, and the remarkable difference with respect to the planets of our Solar System. Traditional theories of planetary formation have been seriously challenged by these discoveries, and there are many aspects that still need to be understood in detail, like planetary migrations (disk-embedded vs planet-planet interactions) and the influence of the metallicity on the planetary formation processes, just to mention some. The heterogeneity of EPs has been analyzed in several papers, and some important trends have been uncovered (e.g. see Zucker & Mazeh 2002; Santos et al. 2003; Udry et al. 2003; Eggenberger et al. 2004; Sozzetti 2004; Fischer & Valenti 2005). On the other hand,

planetary formation is a very complex process, where a number of parameters have important effects, as shown by several theoretical works. It is also likely that some parameters act simultaneously in a complex way, thus motivating the need for a multidimensional approach going beyond the search for simple correlations among individual parameters. In other words, the planetary formation process occurs in a multidimensional space. In addition to Keplerian orbital elements and stellar properties, other relevant parameters may be discovered in the future, as the formation theories improve.

We adopt a multivariate approach to EPs in order to uncover underlying trends which may provide important information about the planet formation processes. The first step is the development of a robust taxonomy for EPs. Taxonomy, just as in other fields of research, may be a precious tool in defining clusters of EPs, which in turn may highlight differences in the formation processes and subsequent evolution.

This will be of particular importance with the increasing number of EP discoveries which is ex-

pected to occur in the near future thanks to several space missions (e.g. CoRoT and Kepler) and ground-based surveys. For the moment, the number of EPs is about 200, which may prevent firm statistical conclusions. Nevertheless, here we propose the guidelines for an EP taxonomy, to be refined as more data become available.

In the next section (2), we describe the parameters used for this study and we perform a statistical approach of the data for dimensional scaling purpose. Then, in section (3), cluster analysis is performed. We caution from the beginning that these analyses -much like all statistical analyses- are not unique, since several different criteria may be used for characterizing the data. There is no a priori best criterion: the choice can indeed vary according to the kind of data under analysis. We shall provide a step-by-step justification for all the choices made. Finally, in section (4), the solution will be discussed along with its physical interpretation.

2. Multivariate analysis and dimensional scaling of EPs

The inputs to our model are the elements provided by the interactive extrasolar planets catalog maintained by J. Schneider¹. These are: planetary projected mass (M_p), orbital period (P), semi-major axis (a), eccentricity (e), inclination (i), stellar mass (M_s), and stellar metallicity ($[\text{Fe}/\text{H}]$). Other possibly important parameters, like stellar spectral type and stellar age, have not been considered at this stage, but will be the subject of further refinements. Only objects having simultaneously estimates for $\{M_p, P, a, e, M_s, [\text{Fe}/\text{H}]\}$ have been used. Notice that the period and semi-major axis are obviously correlated, thus only one of them is used (see the following). We refer to them as the *input variables*². Therefore, each planet can be regarded as a point in a 5-fold space. The following analysis has been carried out in the IDL language, and it is structured so as to be easily updatable as more data become available.

¹<http://exoplanet.eu/>

²We chose to use simply M_p and a instead of performing some transformation of the data prior to the statistical analysis, as done by some authors which made recourse to logarithms, because there is no strong physical reason for that. Anyway, we plan to exploit this possibility in further works.

We consider 183 EPs (updated at 8 November 2006). To them, the Solar System planet Jupiter has been added. This has been done because Jupiter-like bodies are approaching the observability limit in extrasolar planetary systems thanks to recent improvement in the surveys, and also to have a direct comparison with our own Solar System. We decided not to add the other Solar System planets as they are still well below the detection limits. The first step is to perform a statistical analysis in order to find out if there are useless -or less significant- input variables. This is done using principal component analysis (PCA). As this is a standard technique in multivariate data analysis, details will not be discussed here (interested readers may consult Everitt & Dunn 2001). The basic idea of PCA is to combine the input variables in such a way as to show those of most importance. This is done by describing the data with a number of new variables $pc_1 \dots pc_l$ for $l = 5$, ordered in terms of decreasing variance. The pc_i are chosen in such a way as to be uncorrelated with each other. This is done in practice by building an $n \times l$ input data matrix (where n is the number of planets). From this matrix, the $l \times l$ correlation or covariance matrix is computed, where the correlation matrix is more appropriate whenever the input variables are measured with disparate units. The pc_i are eigenvectors for those matrices. Considering that input variables have different units and that some span orders of magnitudes (e.g. M_p) while others span a limited range (e.g. M_s), we opted to perform variable standardization of the input variables, i.e. to scale input variables in such a way as to obtain a mean and variance of 1. This has the advantage of allowing the use of the covariance matrix, for which the eigenvalues (λ_i) represent the portion of the variance of the original data which the corresponding eigenvectors (pc_i) account for. PCA can thus provide a useful means for finding variables of little significance. On the basis of the variance attained by each pc_i we may reject some of them. This procedure has the advantage of using only the variables which are important, allowing a simpler description of the data set with only a minor loss of information.

As a first step, we used PCA to decide whether the period or the semi-major axis is more suitable for the statistical analysis (see also §3.2 on

this point). PCA was then performed on the $\{M_p, P, e, M_s, [\text{Fe}/\text{H}]\}$ and $\{M_p, a, e, M_s, [\text{Fe}/\text{H}]\}$ spaces. The choice was made by requiring that the variance of the resulting pc_i is more concentrated in the first principal components. The 5-fold $\{M_p, a, e, M, [\text{Fe}/\text{H}]\}$ space turned out to be slightly more appropriate. Now, no commonly accepted rules exist for deciding which variables -if any- can be safely thrown away. One criterion suggests keeping variables which account for 70-90% of the total variance (Everitt & Dunn 2001). Thus it seems reasonable to keep only the first three principal components which account for 73% of the total variance. The fact that we can use only 3 principal components allows a graphical representation and a better control of the results. Moreover, dimensional scaling has the effect of simplifying the clustering analysis. This is why we employed PCA, but we are aware it is not strictly necessary for the development of a taxonomy. In fig. 1 the first three principal components are shown.

To the accepted levels of variance we may write the following *decomposition* formulae:

$$\begin{aligned}
 pc_1 &= -0.206 \cdot (M_p - 2.64) - 0.543 \cdot (a - 1.19) - \\
 &\quad 3.417 \cdot (e - 0.25) - 1.823 \cdot (M_s - 1.03) + \\
 &\quad 0.067 \cdot ([\text{Fe}/\text{H}] - 0.1) \\
 pc_2 &= -0.083 \cdot (M_p - 2.64) - 0.030 \cdot (a - 1.19) - \\
 &\quad 0.335 \cdot (e - 0.25) + 3.080 \cdot (M_s - 1.03) + \\
 &\quad 3.921 \cdot ([\text{Fe}/\text{H}] - 0.1) \\
 pc_3 &= 0.090 \cdot (M_p - 2.64) - 0.329 \cdot (a - 1.19) + \\
 &\quad 1.795 \cdot (e - 0.25) - 1.748 \cdot (M_s - 1.03) + \\
 &\quad 2.063 \cdot ([\text{Fe}/\text{H}] - 0.1)
 \end{aligned}$$

where each pc_i is expressed in terms of a linear combination of all the input variables. Notice that $[\text{Fe}/\text{H}]$ has little influence on pc_1 , while a and e basically do not contribute to pc_2 (consider that input variables span different ranges, so for instance, the term containing e in equ. 2 has lower importance than the term involving M_p). These formulae may be used to add new planets into the database, without repeating the PCA (this is useful when we want to add only single objects which do not alter the overall statistics, otherwise PCA has to be repeated).

Finally notice that we also checked for the pres-

ence of overall correlations within the database. We found significant correlation (see also below) between $M_p - e$, $a - e$ and $M_p - a$. However, overall correlations have been widely analyzed elsewhere and will be not discussed here (e.g. Santos et al. 2005, and references therein).

3. Cluster analysis

Cluster analysis is a standard technique used in a variety of research fields from social sciences to geology, engineering and so on. The main purpose of such analysis is to find clusters in a given dataset such that elements belonging to the same cluster have a certain degree of homogeneity, while elements of different clusters have to be as different as possible. As with PCA, there is no unique way of performing the analysis and a number of clustering algorithms are available. The choice of the clustering technique is quite arbitrary and it relies mostly on the kind of description of the data we are interested in. When the number of clusters is not known a priori, as in our case, hierarchical clustering is more suitable, thus we adopt this technique (Everitt et al. 2001). The major advantage of this technique is that it provides a classification which consists of a series of nested partitions, which go from a single cluster containing all objects to n clusters each containing a single object. This process is based on a *proximity* parameter, usually a measure of distance among objects. Moreover, this classification may be represented by a two-dimensional diagram known as a *dendrogram*, which illustrates the nested nature of the hierarchical partition. However, there are a number of possible ways to perform the analysis, and an accurate step-by-step evaluation of the process has to be performed. In the following we refer to the variables used for the clustering (namely the $\{pc_i\}$) as *clustering variables*. The general guidelines for hierarchical cluster analysis are the following (for more details see Everitt et al. 2001):

- standardization of the clustering variables;
- computation of the proximity matrix, that is, evaluate the degree of proximity among dataset members. This is usually done by computing the distance in the clustering space (in our case the 3-fold $\{pc_1, pc_2, pc_3\}$ space). Notice that several metrics may be used for this purpose;

- definition of inter-group proximity measures. These specify the method used to quantify the proximity level of two clusters. Several methods are available, like *single linkage* and *centroid linkage*;
- computation of the distortion of the dendrogram. The dendrogram itself is a representation of the original data, where the separation of two members is specified by the minimum distance between the two clusters which contain the objects. Thus the quality of a dendrogram can be evaluated by comparing the original distance (i.e. in the clustering space) of members with the distance assigned to them by the dendrogram. This is formally done by the so-called *cophenetic coefficient*³ (\hat{c}). It normally ranges from 0.6 to 0.95, where higher values correspond to a lower distortion;
- definition of the best partition. In standard analysis this means stopping the hierarchy at a given distance; in other words to cut a dendrogram at a particular distance (or *height*, h). Again, no unique rule exists to define the best cut. Here we follow the procedure suggested by Mojena (1977), the so-called *upper tail rule*. In detail, we first evaluate the distribution of the heights $N(h)$, then the best cut height is determined by

$$h_\gamma = \bar{h} + \gamma \cdot \sigma_h$$

where γ is a coefficient which ranges from 1.25 to 3.5 (Milligan & Cooper 1985), \bar{h} is the mean of the height distribution and σ_h its standard deviation. A possible way to define the best γ is to find the values of γ for which the maximum separation between two consecutive solutions is achieved;

³To compute \hat{c} proceed as follows. First, compute the distance between two planets (indicated by indices i and j) assigned by the dendrogram. Let d_{ij} be this distance, and d the average value of all d_{ij} . Let r_{ij} be the real distance between planet i and j , and r the average value of all r_{ij} . Thus:

$$\hat{c} = \frac{\sum_i \sum_{j>i} (r_{ij} - r)(d_{ij} - d)}{\left[\sum_i \sum_{j>i} (r_{ij} - r)^2 \sum_i \sum_{j>i} (d_{ij} - d)^2 \right]^{1/2}}$$

- testing of the quality of the solution against the absence of clusters.

3.1. Finding the best solution

First we decided not to standardize the clustering variables as this may reduce the difference among members, making the identification of clusters more difficult. Moreover, as a general rule, the same metrics should be used for the proximity matrix and the inter-group proximity measures. We explored different metrics and the effects of different algorithms of inter-group merging. The metrics used are: Euclidean, City Block, Chebyshev, and correlative (based on the Pearson correlation coefficient). The inter-group algorithms considered are: single linkage, complete linkage, weighted pairwise average and weighted centroid. The full set of possibilities has been investigated by using the cophenetic coefficient and analyzing the corresponding dendrograms. \hat{c} ranged from about 0.55 to 0.84. Although useful, the cophenetic coefficient cannot be the only parameter for finding the best solution; very different hierarchies may have the same \hat{c} . Here, we also considered other features in order to define the best solution. Among them, we first select the dendrograms having $N(h)$ distributions with the lowest variance, i.e. those more peaked for low heights. Then, we required the tails of the $N(h)$ distributions have to be very “discrete” for large heights, that is the solutions with k and $k + 1$ clusters (for low values of k) had to be well separated. Both conditions help to define a robust solution which is closely nested for small heights and stable against errors (e.g. observational errors) on the position of the EPs in the clustering space.

Taking into account these constraints, the best solution was obtained with the Pearson correlation distance⁴ and weighted centroid merging. This solution corresponds to $\hat{c} = 0.83$. According to the upper tail rules, the best cut produces five robust clusters. Remarkably, the interval of heights for which the solution is stable corresponds to 7% of the maximum height (notice that the average separation between two consecutive clusters is of the order of the maximum height divided by n , or $\sim 0.5\%$). The corresponding best solution dendro-

⁴The distance between two items i, j is defined as $d_{ij} = [(1 - \phi)/2]^{1/2}$, where ϕ is the Pearson correlation coefficient.

gram is shown in figure 2. The dendrogram is well structured: for low heights the clusters are closely nested (i.e. small variation of the height results in a significant change in the number of clusters); while for higher values the clusters are well separated.

It is interesting to note that traditional metrics (like the Euclidean) and traditional cluster merging (like single linkage) produce, in general, bad results. It turns out that they are not able to find structures for EPs. This is in agreement with the analysis of Jiang et al. (2006), although it was performed with a very different approach to that adopted here. The main problem of these hierarchies is that either they produce just one or two big clusters and some outliers, or the solution is so nested that the definition of cut-off is too arbitrary and meaningless.

3.2. Testing the solution

Before analyzing in detail the best solution found, we have to check for its robustness against the absence of clusters. We recall that cluster analysis will always produce a solution. The test for the absence of structure is done by an accurate evaluation of the intra-cluster separations. In general, unless we are dealing with data with very well separated clusters, the clusters will tend to have some degree of overlap. The overlap between two clusters can be estimated by comparing the distance of two clusters with respect to their volume in the clustering space. In practice, we estimate the center of each cluster (\vec{c}_i), and its radius (r_i), defined as the sphere which contains a given percentage of the cluster members (both \vec{c}_i and r_i are computed with a Euclidean metric). Thus the degree of overlap between clusters i and j is set to: $\omega_{ij} = (r_i + r_j) / \|\vec{c}_i - \vec{c}_j\|$. Where for $\omega_{ij} < 1$ the clusters i, j are well separated. The overall overlap of the solution is defined as:

$$\omega = \sum_{i>j} \omega_{ij} \quad \text{if } \omega_{ij} > 1.$$

Higher values of ω imply larger overlap. Notice that ω is a cumulative parameter and is sensitive to the number of single intra-cluster overlaps, as it should be. To clarify this point, imagine a solution with a given degree of overlap between two clusters, and another one with the same degree

of overlap but among three clusters. The average degree of overlap will be the same, but the ω of the second solution will be higher than that of the first. Indeed the first solution is better than the second since only two clusters are partially merged. For the best solution, we obtained $\tilde{\omega} = 12.3$. One way of testing the absence of clusters is with Monte Carlo simulations. We then performed a number of simulations (with 10^3 solutions each), generating n random points in the clustering space. The points are generated with a uniform distribution along each axis. Then we run the clustering analysis using the same procedure described before, varying also the volume of the Monte Carlo generated points in the clustering space, and the percentage of objects used for defining the cluster's radii. The probability of obtaining $\omega < \tilde{\omega}$ is less than 10% in all cases. Thus we may safely reject the possibility of the absence of structures. For the sake of completeness, we also perform additional tests to see whether our initial choice of using a instead of P is indeed a good choice in terms of taxonomy. Performing clustering analysis using P instead of a , we obtain a solution which has $\omega = 20$ and is compatible with the absence of structures. A possible explanation of this behavior could be due to the fact that P, a and M_s are related. As a result, the use of the pair a, M_s is better than the pair P, M_s . This further strengthens the case for the use of the semi-major axis.

Moreover, we also tested the solution with respect to the presence of observational errors, which can be very large in some cases. To do this, we generated a random error in the input variables around the nominal values for all the EPs. We then repeated the PCA and cluster analysis of these fictitious samples (one for each of the input variables). The solution obtained has been compared with the best solution. For errors of a few percent, we find that some planets may move to other clusters, but this is limited to a few objects. Increasing the errors, sometimes a cluster may split into two sub-clusters. For errors larger than 10% the solution may alter considerably. In general the best solution does not change much for errors up to $\pm 10\%$ for each of the input variables. This is very important, since it means that the solution is quite stable, in particular considering that we are dealing with projected planetary masses and not real

masses.

The process developed for EP taxonomy is sketched in fig. 4.

4. Analysing the clusters

Our best solution is composed of five robust clusters. In this section we present the properties of each cluster. Figure 3 shows the position of clusters in the clustering space. We checked for inter-correlation among the input variables within each cluster. It is commonly accepted that planets may form in different ways (core accretion vs disk instability), and that their evolution is affected by several parameters (disk density, stellar types, opacity etc). The EP database may reflect such complexity, however the signature of these processes may be blurred in statistical analyses which deal with the whole EP dataset. On the contrary, if cluster separation has something to do with the formation and evolutionary processes and is not just a mere classification, it becomes important to look for trends within each cluster. In the following we report only highly significant (with a 2-tailed probability less than 5%) intra-cluster correlations.

4.1. Cluster $\mathcal{C}1$

Containing 11 EPs (see tables 1 and 2 for a detailed description) this is the least populated cluster. We can define a *prototype* planet, that is the object closest to the center \vec{c}_i of the cluster. The prototype is HD 41004 A b. Figure 5 shows the distribution of the input variables for each cluster. The EPs of this cluster are characterized by a wide range of planetary masses, from about $0.2 M_J$ to $18.4 M_J$. The planetary semi-major axis ranges from 0.018 AU to 1.97 AU. The eccentricities are quite spread, from 0.08 to 0.63. The stellar masses are remarkably sub-solar (except for HD 8574 b which has $1.04 M_\odot$). Finally, star metallicity is very spread, from -0.5 to 0.28 dex. $\mathcal{C}1$ contains several peculiar EPs. HD 41004 B b, HD 162020 b HD 114762 b are very massive planets, with 18.4, 13.7 and $11 M_J$ respectively (see tabs. 1 and 2). The first two are also hot Jupiters (notice that HD 162020 b could be a brown dwarf, according to Udry et al. 2002). This cluster contains 6 EPs in multiple star systems (MSS), see tables 1

and 2 (data on multiple star systems have been taken from Desidera & Barbieri 2006). Moreover HD 41004 B b, HD 162020 b, HD 114762 b and HD 111232 b orbit low mass, low metallicity, stars. Despite this variety, the objects in this cluster have to be considered “similar” in terms of clustering analysis and “different” to the other EPs. We underline that the cluster analysis has been done in the $\{pc_i\}$ space, therefore the input variables may vary considerably within a cluster.

Significant intracluster correlations exist between $M_p - e$ and $M_p - M_s$ (see fig. 6). Notice that M_p is anticorrelated with M_s . This is somehow unexpected as for higher M_s we would expect a higher dust surface density for the protoplanetary disks (Ida & Lin 2005) and hence more massive planets (consider also that here we have sub-solar stellar masses; on this point see also $\mathcal{C}4$). We may argue that this has something to do with the peculiar way these EPs formed, but no firm conclusion can be drawn yet.

4.2. Cluster $\mathcal{C}2$

This cluster contains 46 EPs (see tables 1 and 2). The prototype is HD 69830 c. This cluster is characterized by an M_p distribution with an average of about $1 M_J$ and a standard deviation of $1.2 M_J$, clearly peaked at low masses. Most of the planets have masses below $1.3 M_J$. The semi-major axis distribution is characterized by two distinctive groups, one peaked at very small a and the second, far less numerous, centered at $a \sim 1.6$ AU. The overall distribution has an average of 0.46 AU and a standard deviation of 0.7 AU. Planetary eccentricities are moderate-to-low, 0.11 ± 0.11 , and stellar masses are remarkably sub-solar, $0.83 \pm 0.2 M_\odot$. Star metallicities are around solar, with an average of -0.04 dex, and a standard deviation of 0.22 dex (see fig. 5). Gl 581 b, Gliese 876 b-c-d and GJ 436 b which orbit low mass stars (respectively with 0.31, 0.32 and $0.41 M_\odot$ they are the lowest M_s in the sample) also with low metallicity (respectively -0.33, -0.12, -0.32 dex) belong to this cluster.

$\mathcal{C}2$ contains 17 hot Jupiters (that is 37% of its members), and 4 EPs belong to MSSs (see tables 1 and 2). It also contains 5 transiting EPs (the total number of transiting EPs is 14 -at December 2006- but only 9 are involved in the present analysis; see Burrows et al. 2006). These 5 transiting

EPs do not seem to have any particular properties, except to have the highest stellar ages of the sample (but we warn that those ages may not be well constrained). Finally, $\mathcal{C}2$ contains 13 planets in multiple planet systems (MPS).

The significant intra-cluster correlations are $a - e$ and $a - [\text{Fe}/\text{H}]$ (see fig. 7). The first one is very interesting because a is anti-correlated with e . Thus planets further away from the stars have higher eccentricities. In other words, either the excitation of e is more effective further away from the central star (assuming that planets form in circular orbits) and/or e dumping is more effective for lower a . This result is consistent with tidal circularization of planets with small a , however notice that at $a \sim 0.02$ AU the average e is about 0.1, that is, still considerably non-zero (we caution that low e values could be affected by biases due to fitting procedures, Ford 2005). Moreover, with a notably steep trend, a anti-correlates with $[\text{Fe}/\text{H}]$. Thus either the planetary migration is more pronounced for high $[\text{Fe}/\text{H}]$ (which is in agreement with simulations, e.g. see Livio & Pringle 2003) or giant planets of this cluster may form close to stars (≤ 1 AU) in high metallicity environments. We recall that for $[\text{Fe}/\text{H}] > 0$ the most accredited formation theory is core accretion (Fischer & Valenti 2005; Santos et al. 2005). Notice also that the distribution of the MPS planets in the $a - [\text{Fe}/\text{H}]$ plane is somehow opposite to the overall observed trend: without them the correlation would be even more pronounced. Both trends are very important because, for the first time, they show significant dependence between metallicity and orbital parameters (on the possible existence of a period-metallicity correlation see Sozzetti 2004). These findings also suggest that lower $[\text{Fe}/\text{H}]$ planets tend to have larger orbits, making them difficult to detect (e.g. see Boss 2002). In turn, this may affect the probability of forming planets with respect to the metallicity (Santos et al. 2004; Fischer & Valenti 2005).

4.3. Cluster $\mathcal{C}3$

Containing 48 EPs (see tables 1 and 2) this cluster, along with $\mathcal{C}4$, is the most populated. The prototype is HD 11964 A b, and it contains Jupiter. This cluster is characterized by an M_p distribution peaked at low masses: basically all EPs are below $2.5 M_J$. The semi-major axis dis-

tribution is very peaked at low values: most of the bodies are below 0.25 AU, with a second, less numerous, peak at about 1 AU. Eccentricities are below about 0.3, having an average of 0.096 and a standard deviation of 0.091. Stellar masses span from 0.98 to $1.24 M_\odot$. Metallicities tend to be super-solar and vary from 0.02 to 0.35 dex (see fig 5).

The significant intra-cluster correlations are: $M_p - M_s$, $M_p - [\text{Fe}/\text{H}]$, $a - M_s$, $a - [\text{Fe}/\text{H}]$, $e - [\text{Fe}/\text{H}]$, and $M_s - [\text{Fe}/\text{H}]$. However the first three are due to outliers: without them the correlations do not hold. Therefore they are not considered interesting. On the contrary, the latter three -all involving the metallicity- are robust (see fig. 8). First of all, a is anti-correlated with $[\text{Fe}/\text{H}]$. Thus either the planetary migration is more pronounced for high $[\text{Fe}/\text{H}]$ (see also $\mathcal{C}2$) or planets with lower $[\text{Fe}/\text{H}]$ form at larger distances. A striking result is that Jupiter fits very well in this cluster: its large a would be the result of its formation in a solar-like metallicity disk. Moreover, e is anti-correlated with $[\text{Fe}/\text{H}]$. In other words, higher metallicities correspond to lower eccentricities. Thus either the excitation of e is more effective -or dumping is less effective- for lower metallicities. In order to understand the meaning of these correlations, two further points have to be considered. First, the existence of $a - [\text{Fe}/\text{H}]$ and $e - [\text{Fe}/\text{H}]$ correlations does not imply a correlation between a and e . Indeed they are not correlated to the level of confidence adopted here. Moreover, the members of this cluster have very super-solar metallicities. These correlations, if related to the formation processes, may give important indications about the origin of high eccentricities. Many theories have been proposed (Holman et al. 1997; Murray et al. 2002; Goldreich & Sari 2003; Zakamska & Tremaine 2004; Namouni 2005; Adams & Laughlin 2006; D'Angelo et al. 2006; Fregeau et al. 2006) but none has observational support yet. Here we suggest that the metallicity acts in some way in determining e . For instance, since high $[\text{Fe}/\text{H}]$ produces a faster migration, the low values of e observed for high $[\text{Fe}/\text{H}]$ may be the result of the migration process, e.g. tidal circularization (see also Halbwachs et al. 2005). Alternatively the condition for the pumping up of e during planet-disk interactions (Sari & Goldreich 2004; Matsumura & Pudritz 2006) is not achieved in

high [Fe/H] environments: indeed higher [Fe/H] implies higher disk viscosity and hence a lower probability of e excitation (see equ. 8 and 9 of Sari & Goldreich 2004). If confirmed, these trends suggest that planetary orbital parameters are mainly controlled by disk properties (e.g. metallicity) rather than being affected by *external* factors, like perturbation due to interactions with a companion star or star encounters.

Finally, M_s is anti-correlated with [Fe/H]. It is not easy to understand this correlation, and in particular if it has something to do with the planetary formation process. We note that EPs in this cluster (which are quite confined in terms of a and M_p) orbit stars whose metallicities tend to increase as stellar masses decrease. If we assume that higher M_s implies higher proto-planetary disks masses from which EPs formed, this implies that to form planets in lower metallicity environments a more massive disk is required, in agreement with the core accretion theory.

Eleven EPs are in MSSs (see table 2). It contains also 23 hot Jupiters (48% of the members) and 8 MPS planets. They are well spread and seem not to affect the a -[Fe/H], e -[Fe/H] correlations. However, all MPS planets and most of the hot Jupiters lie above the linear fit in the M_s -[Fe/H] plane. Notice also the MPS planets of this cluster have $e < 0.2$ and [Fe/H] > 0.2 and for this reason they differ from those of $\mathcal{C}2$ (which have $e < 0.3$, [Fe/H] < 0.2) and those of $\mathcal{C}4$ (which have $e > 0.3$).

4.4. Cluster $\mathcal{C}4$

This cluster contains 48 EPs (see tables 1 and 2). The prototype is HD 142022 A b. $\mathcal{C}4$ is characterized by rather flat distributions of the input variables (see fig. 5). In terms of planetary masses, it contains very massive bodies, basically all having $M_p > 2.0 M_J$. Apart from very few exceptions, it contains all the EPs of the dataset having mass greater than $5 M_J$. The average and standard deviations are 5.45 and $3.92 M_J$, respectively. The semi-major axis distribution is also quite flat, ranging from about 0.5 to 5 AU. Mean and standard deviations are 1.98 and 1.27 AU, respectively. Eccentricities are remarkably moderate-to-high, spanning from 0.3 to 0.8 (mean and standard deviation are 0.49 and 0.18, respectively). Stellar masses are mainly around one solar mass, with a slight overabundance of

super-solar mass objects. Mean and standard deviations are 1.06 and $0.13 M_\odot$, respectively. Metallicities span from -0.25 to 0.3 dex, having an average and standard deviations of 0.14 and 0.17 dex, respectively. Thus despite its wide distribution of metallicities, EPs are mainly super-solar.

Two significant correlations exist for this cluster: $M_p - e$ and $M_p - M_s$ (see fig. 9). The first implies that lower mass EPs have higher e , thus the mechanisms for the pumping-up of the eccentricity are more active in low mass planets, at least for the high semi-major axes and moderate positive metallicities of this cluster. Moreover, EP masses are correlated with stellar masses. This may confirm the fact that higher M_s implies larger proto-planetary disk surface density and hence larger M_p (Ida & Lin 2005).

$\mathcal{C}4$ contains 12 EPs in MSSs and 12 in MPS (see tables 1 and 2). Notice that the MSS planets may be responsible of the $M_p - e$ correlation as many of them have low M_p and high e .

4.5. Cluster $\mathcal{C}5$

This cluster contains 31 EPs (see tables 1 and 2), and the prototype is HD 117207 b. Planetary masses have intermediate values, with a mean of $2.16 M_J$ and a standard deviation of $1.24 M_J$, respectively. The semi-major axis distribution is rather flat spanning from 0.37 to 3 AU, with a few bodies around 4 AU. Eccentricities are peaked at 0.2-0.3, and range from 0.2 to 0.5. Stellar masses are super-solar, having mean and standard deviation of 1.22 and $0.21 M_\odot$, respectively. Stellar metallicities are also remarkably super-solar, having mean and standard deviation of 0.15 and 0.15 dex (see fig. 5).

The formally significant correlations are: $M_p - M_s$, $M_p - [\text{Fe}/\text{H}]$ and $a - e$. However they are all due to outlier planets and thus cannot be considered as real (notice that if we do not consider the outliers, the correlation $a - e$ is very close to the 5% significance level, thus it may become significant as more objects are added to this cluster by future discoveries).

It contains 7 EPs in MSSs and only one hot Jupiter (namely, HD 118203 b). It is interesting to understand why this hot Jupiter is in this cluster. The peculiarity of HD 118203 b is that it has the highest eccentricity (0.309) among hot Jupiters.

Notice that HD 185269 b (in $\mathcal{C}3$) also has a very high eccentricity of 0.3. All the other input variables are the same, except for the planetary mass. HD 118203 b with a mass of $2.13 M_p$ is one of the most massive hot Jupiters. This explains why HD 118203 b has been put in this cluster. This cluster contains 13 EPs in MPS.

Despite the lack of any correlation, few comments may be added to uncover the nature of this cluster. $\mathcal{C}4$ and $\mathcal{C}5$ have some similar traits. They have spread and rather flat distributions of input variables. Moreover, both have large semi-major axes and eccentricities. However, $\mathcal{C}5$ contains objects with higher stellar masses, lower eccentricities and lower masses than $\mathcal{C}4$.

5. Discussion and conclusion

In this paper we develop the basis for an extrasolar planet taxonomy. We use as many inputs as possible for this analysis, in particular the planetary mass, semi-major axis, eccentricity, stellar mass and stellar metallicity. We identify the best procedure to follow: a multivariate statistical analysis (PCA) to find the most important variables, and then hierarchical cluster analysis. We analyze the solutions via canonical means (through the cophenetic coefficient) and by analysis of the distribution of the dendrogram's heights. The best result is achieved with non traditional metric and merging algorithms, namely the Pearson correlation metric and weighted centroid cluster merging. We reject the absence of clustering structure with Monte Carlo simulations, and also test the stability of the solution against observational errors of the input variables. The procedure we followed is able to provide a robust extrasolar planet taxonomy even if the number of planets is still low. The general traits of the taxonomy developed here will be updated as more planets become available.

Our best solution consists of five clusters. We discuss their properties with respect to the physically relevant input variables. We show the importance of including the environmental variables (M_s and $[\text{Fe}/\text{H}]$) to discriminate between otherwise similar planets; and also to merge together different bodies (like EP in MSSs and orbiting single stars). For instance, we were able to divide the hot Jupiters into -at least- 2 main groups (see tab. 1). This division is mainly due to the stellar mass and

metallicity. Those belonging to $\mathcal{C}3$ basically orbit around stars with super-solar masses and high metallicities; those of $\mathcal{C}2$ orbit mostly sub-solar mass stars with moderate (both positive and negative) metallicities. This may reflect differences in the formation processes of these EPs.

Jupiter belongs to cluster $\mathcal{C}3$. Much as been speculated about the similarity of our Solar System and extrasolar systems (e.g. Beer et al. 2004), in particular concerning the formation histories. With the help of cluster analysis we may identify those EPs which are more similar -in the 3-fold clustering space- to Jupiter. We suggest that the actual large semi-major axis of Jupiter is the result of its formation in a solar-like metallicity disk.

We also analyzed the intra-cluster correlations, since this may provide important information about the formation and evolution of bodies within a cluster. This is crucial in order to uncover information which may be hidden in the “blind” statistical analysis performed on the whole EP database. The most important correlations found are those for $\mathcal{C}2$, $\mathcal{C}3$ and $\mathcal{C}4$ (see tab. 1). Remarkably, for $\mathcal{C}2$ and $\mathcal{C}3$ we find important trends between metallicity and orbital parameters. We find that $[\text{Fe}/\text{H}]$ has very important effects on the semi-major axis (and thus on the migration processes) and the eccentricity. It may also happen that the same variables correlate in an opposite way between two different clusters (see the $M_p - M_s$ correlations for $\mathcal{C}1$ and $\mathcal{C}4$). Moreover, we also studied the distribution of planets in multiple star systems in each cluster. They do not seem to play a particular role in the corresponding cluster correlations. Similar considerations apply also for multiple planet systems.

In addition to these main five clusters, we may see the position of the pulsar planets in the clustering space. Obviously these planets were not included in the previous analysis because we do not have M_s and $[\text{Fe}/\text{H}]$. However we may use as test values $M_s = 10 M_\odot$ for the progenitors of both PSR 1257+12 and PSR B1620-26. As for the metallicity we assume 0 and -1.05 (the first is an indicative value, the latter is the average for M4 stars), respectively. Using the formule (1), (2) and (3), we find that these planets are very far from all the other EPs in the clustering space, and hence for each pulsar we have a single cluster. This is consistent with the very likely different ori-

gin of the pulsar planets with respect to other EPs.

The author wish to thank C. Barbieri for a careful reading of the paper and financial support. The paper has been funded on MIUR grant PRIN 2006. Many thanks to S. Ortolani and P. Paolicchi for helpful comments and discussion which improved the quality of the paper, and to the anonymous referee for useful comments. I wish to also thank N. Schneider (on sabbatical at the University of Padova) for discussions. Thanks to S. Magrin for IDL support and M. Clemens for corrections to the English.

REFERENCES

- Adams, F. C., & Laughlin, G. 2006, *ApJ*, 649, 992
- Beer, M. E., King, A. R., Livio, M., & Pringle, J. E. 2004, *MNRAS*, 354, 763
- Boss, A. P. 2002, *ApJ*, 567, L149
- Burrows, A., Hubeny, I., Budaj, J., & Hubbard, W. B. 2006, *ArXiv Astrophysics e-prints*, arXiv:astro-ph/0612703
- D'Angelo, G., Lubow, S. H., & Bate, M. R. 2006, *ApJ*, 652,
- Desidera, S., & Barbieri, M. 2006, *ArXiv Astrophysics e-prints*, arXiv:astro-ph/0610623
- Eggenberger, A., Udry, S., & Mayor, M. 2004, *A&A*, 417, 353
- Everitt, B.S., & Dunn, G. 2001, *Applied multivariate data analysis*, second edition, Arnold Ed., London
- Everitt, B.S., Landau, S., & Leese, Morven. 2001, *Cluster analysis*, fourth edition, Arnold Ed., London
- Fischer, D. A., & Valenti, J. 2005, *ApJ*, 622, 1102
- Ford, E. B. 2005, *AJ*, 129, 1706
- Fregeau, J. M., Chatterjee, S., & Rasio, F. A. 2006, *ApJ*, 640, 1086
- Goldreich, P., & Sari, R. 2003, *ApJ*, 585, 1024
- Halbwachs, J. L., Mayor, M., & Udry, S. 2005, *A&A*, 431, 1129
- Holman, M., Touma, J., & Tremaine, S. 1997, *Nature*, 386, 254
- Ida, S., & Lin, D. N. C. 2005, *ApJ*, 626, 1045
- Jiang, I.-G., Yeh, L.-C., Hung, W.-L., & Yang, M.-S. 2006, *MNRAS*, 370, 1379
- Livio, M., & Pringle, J. E. 2003, *MNRAS*, 346, L42
- Mayor, M., & Queloz, D. 1995, *Nature*, 378, 355
- Matsumura, S., & Pudritz, R. E. 2006, *MNRAS*, 365, 572
- Milligan, G.W., & Cooper, M.C. 1985, *Psychometrika*, 50, 159
- Mojena, R. 1977, *Computer Journal*, 20, 359
- Murray, N., Paskowitz, M., & Holman, M. 2002, *ApJ*, 565, 608
- Namouni, F. 2005, *AJ*, 130, 280
- Santos, N. C., Benz, W., & Mayor, M. 2005, *Science*, 310, 251
- Santos, N. C., Israelian, G., & Mayor, M. 2004, *A&A*, 415, 1153
- Santos, N. C., Israelian, G., Mayor, M., Rebolo, R., & Udry, S. 2003, *A&A*, 398, 363
- Sari, R., & Goldreich, P. 2004, *ApJ*, 606, L77
- Sozzetti, A. 2004, *MNRAS*, 354, 1194
- Udry, S., Mayor, M., & Santos, N. C. 2003, *A&A*, 407, 369
- Udry, S., Mayor, M., Naef, D., Pepe, F., Queloz, D., Santos, N. C., & Burnet, M. 2002, *A&A*, 390, 267
- Zakamska, N. L., & Tremaine, S. 2004, *AJ*, 128, 869
- Zucker, S., & Mazeh, T. 2002, *ApJ*, 568, L113

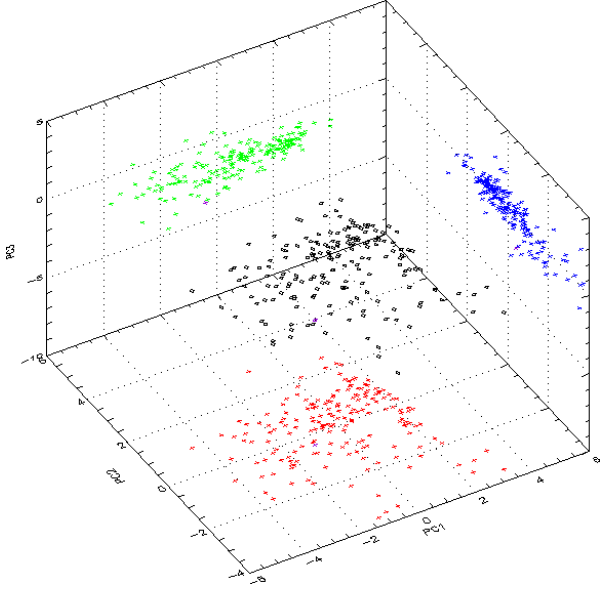


Fig. 1.— Distribution of the data in the 3-fold clustering space.

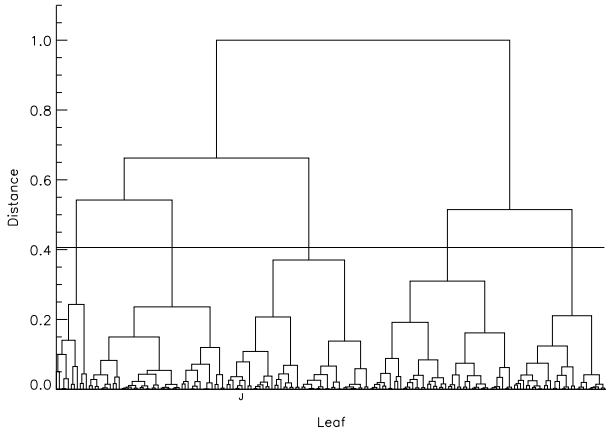
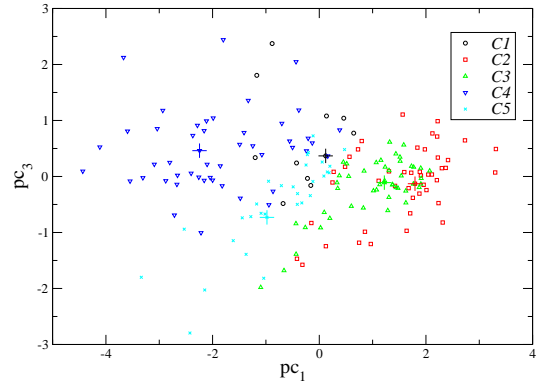
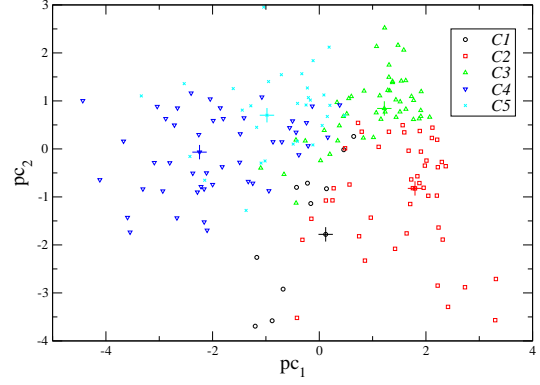


Fig. 2.— Dendrogram of the best solution. Jupiter position is also reported. The horizontal line corresponds to the best cut (see text).

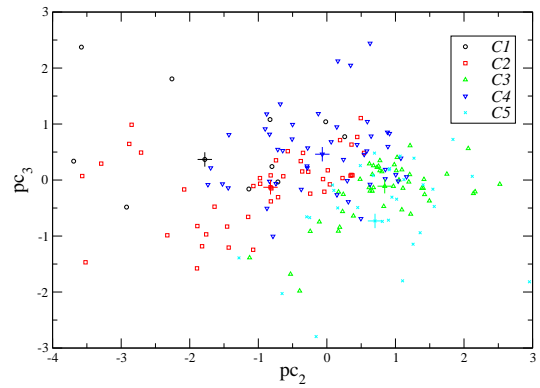


Fig. 3.— Distribution of the clusters in the clustering space projected onto the $pc_1 - pc_2$, $pc_1 - pc_3$ and $pc_2 - pc_3$ planes. Large pluses indicate the prototype planet of each cluster (see text).

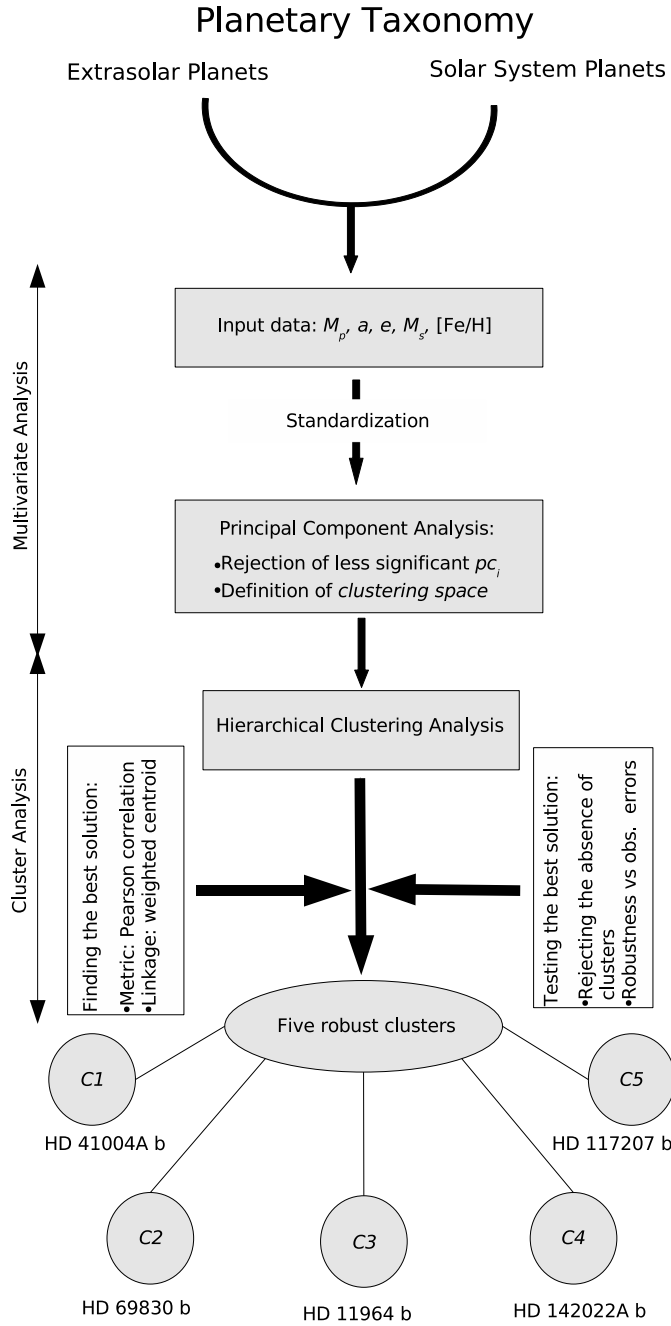


Fig. 4.— Guidelines for the planetary taxonomy developed in this paper. As for the Solar System, only Jupiter has been included in this analysis so far (see text for further detail). Below each cluster the corresponding prototype is reported.

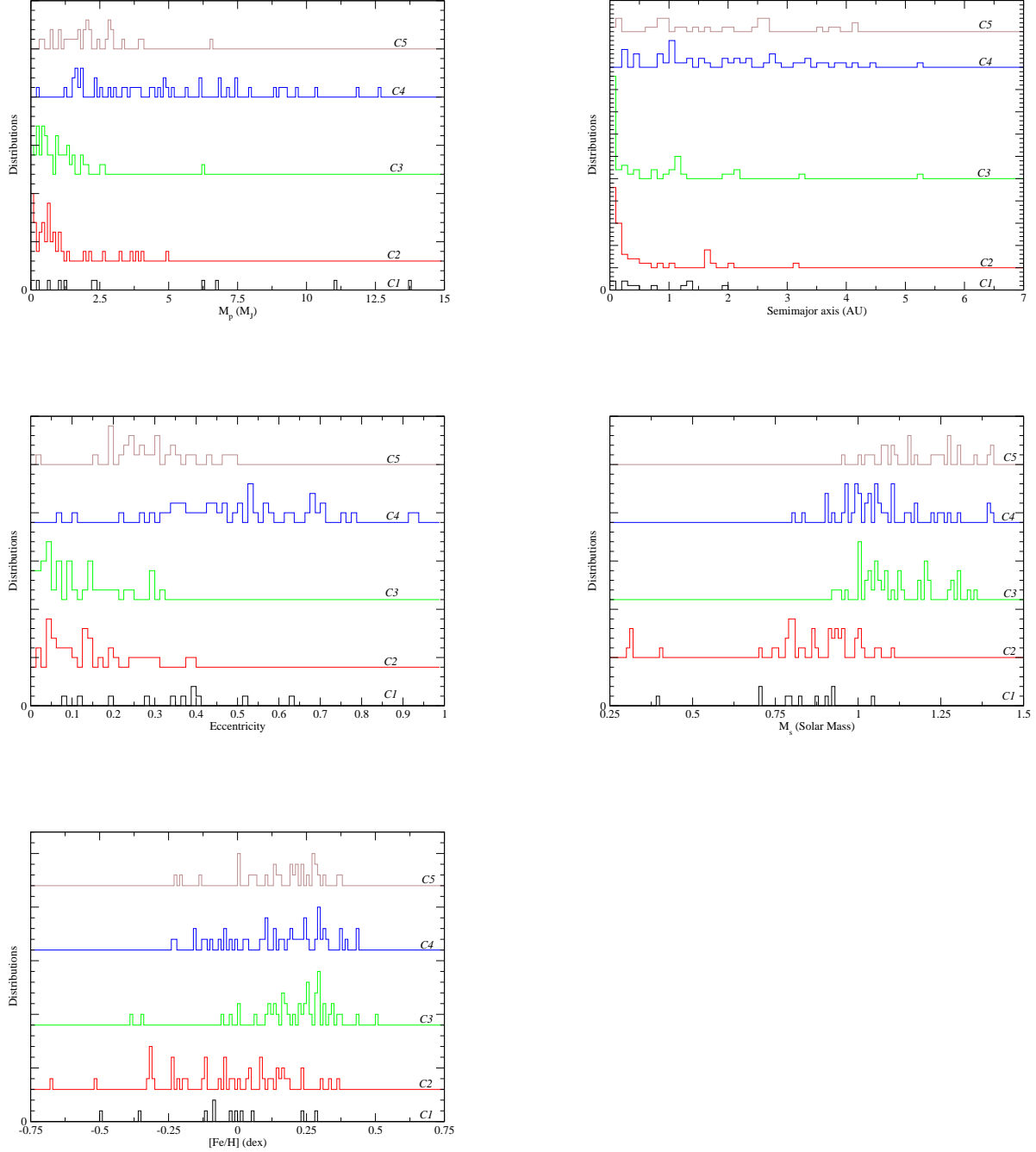


Fig. 5.— Comparison of the distributions of the input variables for each cluster. Within each panel the distributions have been vertically shifted for clarity. The vertical distance between two consecutive major ticks corresponds to 5 units.

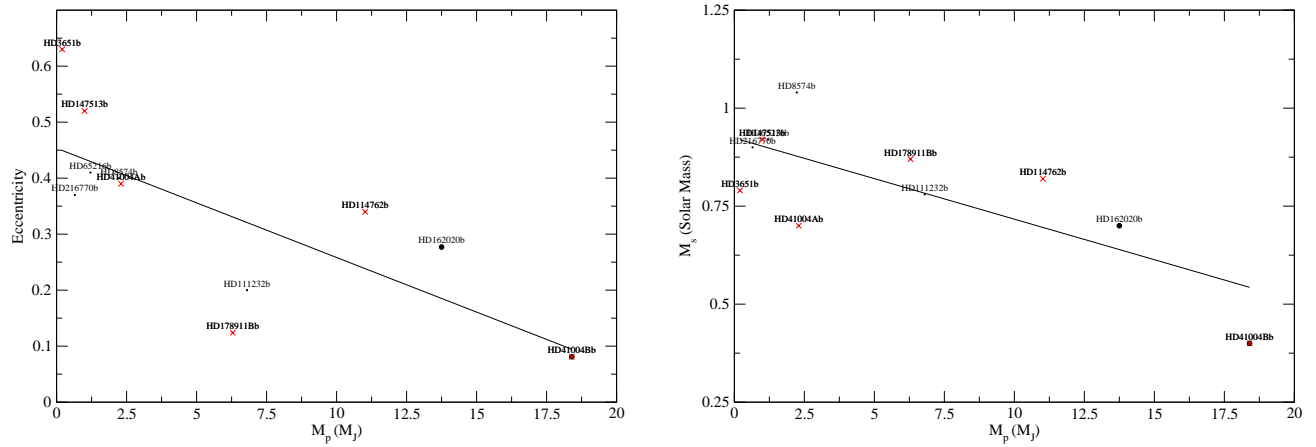


Fig. 6.— Significant correlations within cluster $\mathcal{C}1$. The solid line is the best linear fit. Black circles indicate hot Jupiters, while crosses correspond to planets in multiple star systems.

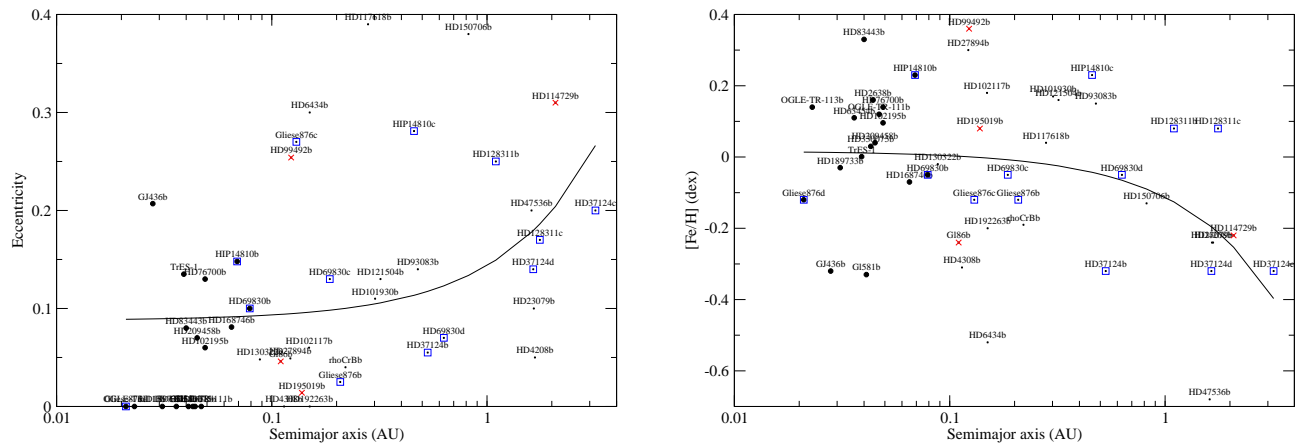


Fig. 7.— Significant correlations within cluster $\mathcal{C}2$. The solid line is the best linear fit. Black circles indicate hot Jupiters, crosses correspond to MSS planets and squares to MPS planets (notice the x-axis log scale).

TABLE 1

RELEVANT DATA FOR EXTRASOLAR PLANET CLUSTERS. CORR: ALL SIGNIFICANT INTRACLUSTER CORRELATIONS, I.E. HAVING 2-TAILED PROBABILITY LESS THEN 5%. THOSE OF $\mathcal{C}2$, $\mathcal{C}3$ AND $\mathcal{C}4$ ARE THE MOST IMPORTANT ONES. WE SHOW THEM IN THE FIGS. 7, 8, AND 9. HT: HOT JUPITERS. T: TRANSITING PLANETS. MSS: PLANETS IN MULTIPLE STAR SYSTEMS. MPS: MULTIPLE PLANETARY SYSTEMS. SS: SOLAR SYSTEM PLANETS.

Cluster	Prototype	Members	Corr	HJ	T	MSS	MPS	SS
$\mathcal{C}1$	HD 41004 A b	11	$M_p - e, M_p - M_s$	2	-	6	-	
$\mathcal{C}2$	HD 69830 c	46	$a - e, a - [\text{Fe}/\text{H}]$	17	5	4	13	
$\mathcal{C}3$	HD 11964 b	48	$a - [\text{Fe}/\text{H}], e - [\text{Fe}/\text{H}], M_s - [\text{Fe}/\text{H}]$	23	4	11	8	Jupiter
$\mathcal{C}4$	HD 142022 A b	48	$M_p - e, M_p - M_s$	-	-	12	12	
$\mathcal{C}5$	HD 117207 b	31	-	1	-	7	13	

TABLE 2

SUPPLEMENTARY MATERIAL: DETAILS ON EXTRASOLAR PLANET CLUSTERS. FOR EACH PLANET WE REPORT THE MASS (M_J), SEMI-MAJOR AXIS (AU), PERIOD (DAYS), ECCENTRICITY, STELLAR MASS (M_\odot), METALLICITY, AND THE FIRST THREE PRINCIPAL COMPONENTS. PLANETS IN BOLD ARE PROTOTYPES. PLANETS IN MULTIPLE STAR SYSTEMS, MULTIPLE PLANET SYSTEMS, TRANSITING, HOT JUPITERS ARE ALSO INDICATED.

Planet	M_p	a	P	e	M_s	[Fe/H]	pc_1	pc_2	pc_3
<i>Cluster C1</i>									
HD147513b [†]	1.000	1.260	538.33	0.520	0.920	-0.030	-0.426	-0.801	0.241
HD162020b ^h	13.750	0.072	8.36	0.277	0.700	0.010	-1.171	-2.260	1.806
HD178911Bb [†]	6.292	0.320	70.64	0.124	0.870	0.280	0.459	-0.017	1.041
HD41004Bb ^{v,h,†}	18.400	0.018	1.33	0.081	0.400	-0.010	-0.883	-3.580	2.373
HD3651b [†]	0.200	0.284	62.19	0.630	0.790	0.050	0.135	-0.829	1.080
HD216770b	0.650	0.460	120.08	0.370	0.900	0.230	0.646	0.260	0.774
HD8574b	2.230	0.760	237.07	0.400	1.040	-0.090	-0.221	-0.714	-0.034
HD114762b [†]	11.020	0.300	65.86	0.340	0.820	-0.500	-1.201	-3.693	0.337
HD111232b	6.800	1.970	1138.84	0.200	0.780	-0.360	-0.678	-2.921	-0.483
HD41004Ab[†]	2.300	1.310	653.56	0.390	0.700	-0.090	0.120	-1.780	0.368
HD65216b	1.210	1.370	610.27	0.410	0.920	-0.120	-0.159	-1.138	-0.160
<i>Cluster C2</i>									
HD121504b	0.890	0.320	66.09	0.130	1.000	0.160	1.306	0.358	0.092
HIP14810c [‡]	0.951	0.458	113.73	0.281	0.990	0.230	0.727	0.542	0.484
HD102117b	0.140	0.149	21.55	0.060	0.950	0.180	1.885	0.373	0.084
HD76700b ^h	0.197	0.049	3.96	0.130	1.000	0.140	1.594	0.345	0.078
HD209458b ^{h,t}	0.690	0.045	3.47	0.070	1.010	0.040	1.675	-0.037	-0.208
HD2638b ^h	0.480	0.044	3.49	-0.000	0.930	0.160	2.112	0.228	0.035
HD195019b [†]	3.670	0.138	18.16	0.014	1.060	0.080	1.114	0.043	-0.077
HD23079b	2.610	1.650	737.31	0.100	1.100	-0.240	0.124	-1.075	-1.245
HD102195b ^h	0.488	0.049	4.12	0.060	0.926	0.096	1.906	-0.056	0.017
HD330075b ^h	0.760	0.043	3.34	-0.000	0.950	0.030	2.010	-0.243	-0.243
HD4208b	0.800	1.670	817.08	0.050	0.930	-0.240	0.966	-1.432	-1.206
HD27894b	0.620	0.122	17.97	0.049	0.750	0.300	2.211	0.192	0.713
HD4308b	0.047	0.114	15.43	-0.000	0.830	-0.310	2.314	-1.889	-0.822
HD37124d [‡]	0.600	1.640	803.93	0.140	0.910	-0.320	0.747	-1.820	-1.183
HD69830c[‡]	0.038	0.186	31.59	0.130	0.860	-0.050	1.795	-0.822	-0.129
HD37124b [‡]	0.610	0.530	147.69	0.055	0.910	-0.320	1.638	-1.760	-0.970
HD69830b ^{h,‡}	0.033	0.079	8.66	0.100	0.860	-0.050	1.957	-0.809	-0.148
HD189733b ^{v,h,t}	1.150	0.031	2.26	-0.000	0.800	-0.030	2.205	-0.973	-0.066
OGLE-TR-113b ^{v,h,t}	1.320	0.023	1.43	-0.000	0.780	0.140	2.223	-0.381	0.338
HD192263b	0.720	0.150	23.86	-0.000	0.790	-0.200	2.236	-1.638	-0.476
TrES-1 ^{h,t}	0.610	0.039	3.05	0.135	0.870	0.001	1.725	-0.636	0.067
HD117618b	0.190	0.280	52.81	0.390	1.050	0.040	0.484	0.013	0.174
HD130322b	1.080	0.088	10.72	0.048	0.790	-0.020	2.044	-0.976	0.034
HD101930b	0.300	0.302	70.46	0.110	0.740	0.170	1.980	-0.348	0.484
HD168746b ^h	0.230	0.065	6.31	0.081	0.920	-0.070	1.878	-0.712	-0.306
OGLE-TR-111b ^{h,t}	0.530	0.047	4.11	-0.000	0.820	0.120	2.298	-0.272	0.148
HD69830d [‡]	0.058	0.630	196.95	0.070	0.860	-0.050	1.755	-0.817	-0.381
rhoCrBb	1.040	0.220	38.65	0.040	0.950	-0.190	1.705	-1.148	-0.658
HD37124c [‡]	0.683	3.190	2180.82	0.200	0.910	-0.320	-0.316	-1.894	-1.577
HD83443b ^h	0.410	0.040	3.29	0.080	0.790	0.330	2.122	0.443	0.769
HD63454b ^h	0.380	0.036	2.79	-0.000	0.800	0.110	2.371	-0.360	0.153
HD114729b [†]	0.820	2.080	1135.74	0.310	0.930	-0.220	-0.148	-1.455	-0.831
HD93083b	0.370	0.477	143.79	0.140	0.700	0.150	1.840	-0.570	0.515
HD6434b	0.480	0.150	21.21	0.300	1.000	-0.520	0.856	-2.327	-0.987
G1581b ^h	0.056	0.041	5.45	-0.000	0.310	-0.330	3.299	-3.568	0.071
Gliese876d ^{v,h,‡}	0.023	0.021	1.94	-0.000	0.320	-0.120	3.312	-2.710	0.490
G186b [†]	4.010	0.110	14.96	0.046	0.790	-0.240	1.421	-2.081	-0.168
HD99492b [†]	0.109	0.123	17.88	0.254	0.780	0.360	1.564	0.494	1.106
GJ436b ^h	0.067	0.028	2.64	0.207	0.410	-0.320	2.414	-3.291	0.293
Gliese876b [‡]	1.935	0.208	61.00	0.025	0.320	-0.120	2.732	-2.882	0.645
HIP14810b ^{h,‡}	3.840	0.069	6.67	0.148	0.990	0.230	0.796	0.359	0.633
HD47536b	4.960	1.610	767.70	0.200	0.940	-0.680	-0.418	-3.520	-1.469

TABLE 2—Continued

Planet	M_p	a	P	e	M_s	[Fe/H]	pc_1	pc_2	pc_3
Gliese876c [‡]	0.560	0.130	30.24	0.270	0.320	-0.120	2.220	-2.848	0.987
HD150706b	1.000	0.820	279.61	0.380	0.940	-0.130	0.248	-1.072	-0.107
HD128311b [‡]	2.180	1.099	469.89	0.250	0.800	0.080	0.567	-0.742	0.352
HD128311c [‡]	3.210	1.760	951.71	0.170	0.800	0.080	0.270	-0.820	0.083
<i>Cluster C3</i>									
HD188015b [†]	1.260	1.190	456.01	0.150	1.080	0.290	0.552	1.051	0.003
OGLE-TR-132b ^{v,h,t}	1.190	0.031	1.68	-0.000	1.350	0.430	1.225	2.522	-0.074
HD134987b	1.580	0.780	245.38	0.240	1.050	0.230	0.452	0.679	0.257
HD224693b	0.710	0.233	35.61	0.050	1.330	0.343	1.074	2.136	-0.239
Jupiter	1.000	5.203	4332.80	0.048	1.000	0.000	-1.098	-0.397	-1.980
HD73526c [‡]	2.500	1.050	388.67	0.140	1.020	0.280	0.516	0.732	0.227
GammaCepheib [†]	1.430	1.940	908.07	0.200	1.180	0.000	-0.262	0.168	-0.911
HD185269b ^h	0.940	0.077	6.90	0.300	1.280	0.110	0.333	0.970	-0.111
HD70642b	2.000	3.300	2187.59	0.100	1.000	0.160	-0.437	0.187	-0.842
HD149026b ^{h,t}	0.360	0.042	2.76	-0.000	1.300	0.360	1.476	2.162	-0.209
HD208487b	0.450	0.490	109.86	0.320	1.300	-0.060	0.093	0.387	-0.641
HD27442b [†]	1.280	1.180	427.19	0.070	1.200	0.200	0.602	1.093	-0.531
HD88133b ^h	0.220	0.047	3.40	0.110	1.200	0.340	1.308	1.750	0.107
BD-103166b ^h	0.480	0.046	3.43	0.070	1.100	0.500	1.584	2.061	0.564
HD68988b ^h	1.900	0.071	6.30	0.140	1.200	0.240	0.840	1.208	0.098
HD52265b	1.130	0.490	117.80	0.290	1.130	0.110	0.377	0.484	0.014
HD107148b	0.210	0.269	48.15	0.050	1.120	0.314	1.538	1.416	0.012
HD109749b ^{h,†}	0.280	0.064	5.33	0.010	1.200	0.250	1.622	1.425	-0.258
HD217107b ^{h,‡}	1.330	0.073	7.13	0.132	1.020	0.370	1.320	1.213	0.614
HD149143b ^h	1.330	0.053	4.05	0.016	1.210	0.260	1.374	1.407	-0.146
HD86081b ^h	1.500	0.039	2.56	0.008	1.210	0.257	1.373	1.384	-0.147
HD160691e [‡]	0.522	0.921	310.59	0.067	1.080	0.280	1.134	1.109	-0.145
UpsilonAndb ^{h,†,‡}	0.690	0.059	4.59	0.029	1.300	0.130	1.285	1.222	-0.608
HD104985b	6.300	0.780	205.04	0.030	1.500	-0.350	-0.661	-0.530	-1.680
HD179949b ^h	0.950	0.045	3.08	0.022	1.280	0.220	1.305	1.495	-0.372
55Cnc ^{h,†,‡}	0.045	0.038	2.67	0.174	1.030	0.290	1.437	1.024	0.404
HD75289b ^h	0.420	0.046	3.52	0.054	1.050	0.290	1.729	1.094	0.184
HD164922b	0.360	2.110	1154.49	0.050	0.940	0.170	0.827	0.229	-0.562
HD73256b ^h	1.870	0.037	2.53	0.030	1.050	0.290	1.517	0.983	0.274
HD99109b	0.502	1.105	439.84	0.090	0.930	0.315	1.235	0.772	0.169
HD114783b	0.990	1.200	500.34	0.100	0.920	0.330	1.068	0.754	0.248
OGLE-TR-10b ^{h,t}	0.630	0.042	2.85	-0.000	1.180	0.120	1.624	0.829	-0.470
HD160691d ^{h,‡}	0.044	0.090	9.49	-0.000	1.080	0.280	1.911	1.195	-0.034
55Cncb ^{†,‡}	0.784	0.115	14.03	0.020	1.030	0.290	1.770	1.012	0.168
HAT-P-1b ^{h,t}	0.530	0.055	4.46	0.090	1.120	0.130	1.440	0.661	-0.197
47Umab	2.600	2.110	1101.77	0.049	1.030	0.060	0.198	-0.110	-0.747
HD20367b	1.070	1.250	500.32	0.230	1.040	0.100	0.346	0.170	-0.212
HD10647b	0.910	2.100	1074.16	0.180	1.070	-0.030	0.025	-0.243	-0.916
HD11964b[†]	0.110	0.229	37.74	0.150	1.125	0.170	1.220	0.843	-0.110
HD108874b	1.360	1.051	393.31	0.070	1.000	0.140	1.016	0.239	-0.255
HD16141b [†]	0.230	0.350	75.62	0.210	1.000	0.220	1.156	0.620	0.290
51Pegb ^h	0.468	0.052	4.21	-0.000	1.060	0.160	1.873	0.629	-0.196
HD212301b ^{v,h}	0.450	0.036	2.43	-0.000	1.050	0.180	1.905	0.679	-0.134
HD187123b ^h	0.520	0.042	3.05	0.030	1.060	0.160	1.765	0.615	-0.134
HD46375b ^{h,†}	0.249	0.041	3.03	0.040	1.000	0.250	1.903	0.802	0.150
HD49674b ^h	0.110	0.057	4.94	0.160	1.000	0.250	1.513	0.773	0.348
HD190360c ^{†,‡}	0.057	0.128	17.07	0.010	0.960	0.240	2.070	0.663	0.100
HD196885b	1.840	1.120	383.91	0.300	1.270	-0.390	-0.434	-1.127	-1.387
<i>Cluster C4</i>									
HD45350b	1.790	1.920	961.39	0.778	1.020	0.290	-1.989	0.590	1.043

TABLE 2—Continued

Planet	M_p	a	P	e	M_s	[Fe/H]	pc_1	pc_2	pc_3
HD74156c [‡]	6.170	3.400	2228.53	0.583	1.050	0.130	-3.093	-0.286	0.217
HD142415b	1.620	1.050	386.94	0.500	1.030	0.210	-0.556	0.440	0.632
HD50554b	4.900	2.380	1276.02	0.420	1.100	0.020	-1.820	-0.374	-0.168
HD142022Ab[†]	4.400	2.800	1716.36	0.570	0.990	0.190	-2.245	-0.067	0.461
HD30177b	9.170	3.860	2829.03	0.300	0.950	0.250	-2.803	-0.291	0.250
HD136118b	11.900	2.300	1138.96	0.370	1.240	-0.065	-3.307	-0.836	-0.024
HD39091b	10.350	3.290	2069.02	0.620	1.100	0.090	-4.114	-0.644	0.525
HD4203b	1.650	1.090	403.43	0.460	1.060	0.220	-0.501	0.582	0.518
HD89744b [†]	7.990	0.890	258.49	0.670	1.400	0.180	-3.038	0.883	0.853
14Herb	4.640	2.770	1770.69	0.369	0.900	0.430	-1.411	0.645	0.784
55Cnc ^{†,‡}	0.217	0.240	42.31	0.440	1.030	0.290	0.383	0.914	0.830
HD190228b	4.990	2.310	1122.69	0.430	1.300	-0.240	-2.217	-0.786	-1.005
HD38529c ^{†,‡}	12.700	3.680	2177.65	0.360	1.390	0.313	-4.434	1.004	0.094
HD160691c [‡]	3.100	4.170	2988.87	0.570	1.080	0.280	-2.879	0.630	-0.078
HD122430b	3.710	1.020	318.75	0.680	1.390	-0.050	-2.259	0.297	-0.013
HD92788b	3.860	0.970	338.35	0.270	1.060	0.240	-0.240	0.544	0.456
HD213240b [†]	4.500	2.030	954.79	0.450	1.220	0.230	-1.855	0.853	0.188
HD217107c [‡]	2.500	4.410	3345.49	0.537	1.020	0.370	-2.658	0.851	0.021
55Cncd ^{†,‡}	3.920	5.257	4330.22	0.327	1.030	0.290	-2.716	0.496	-0.690
HD66428b	2.820	3.180	1932.63	0.465	1.146	0.310	-2.044	1.039	-0.019
HD10697b	6.120	2.130	1079.77	0.110	1.100	0.150	-0.867	0.147	-0.265
HD190360b ^{†,‡}	1.502	3.920	2891.20	0.360	0.960	0.240	-1.481	0.313	-0.389
HD183263b	3.690	1.520	631.87	0.380	1.170	0.300	-1.076	1.079	0.389
HD23596b	7.190	2.720	1450.07	0.314	1.270	0.320	-2.403	1.162	0.057
HD12661b [‡]	2.300	0.830	266.74	0.350	1.070	0.293	-0.131	0.890	0.598
16CygBb [†]	1.680	1.680	798.74	0.689	0.990	0.080	-1.492	-0.280	0.572
HD2039b	4.850	2.190	1193.00	0.680	0.980	0.100	-2.371	-0.507	0.731
HD80606b [†]	3.410	0.439	111.79	0.927	0.900	0.430	-1.800	0.630	2.441
HD202206b [‡]	17.400	0.830	255.72	0.435	1.150	0.370	-3.670	0.160	2.124
HD33564b	9.100	1.100	375.61	0.340	1.250	-0.120	-1.999	-0.743	-0.066
HD20782b [†]	1.800	1.360	578.82	0.920	1.000	-0.050	-2.159	-0.836	0.817
HD222582b [†]	5.110	1.350	571.55	0.760	1.000	-0.010	-2.285	-0.900	0.912
HD28185b	5.700	1.030	382.70	0.070	0.990	0.240	0.160	0.242	0.365
HD106252b	6.810	2.610	1498.43	0.540	1.050	-0.160	-2.669	-1.439	-0.141
HD168443c [‡]	16.870	2.840	1769.45	0.222	0.960	0.100	-3.595	-1.429	0.809
HIP75458b	8.820	1.275	511.15	0.712	1.050	0.030	-2.934	-0.878	1.179
HD141937b	9.700	1.520	681.35	0.410	1.000	0.160	-2.115	-0.501	0.991
HD33636b	9.280	3.560	2454.89	0.530	0.990	-0.130	-3.547	-1.735	-0.083
HD74156b [‡]	1.860	0.294	56.78	0.636	1.050	0.130	-0.702	0.145	0.947
EpsilonEridanib	1.550	3.390	2500.25	0.702	0.830	-0.100	-2.158	-1.523	-0.070
HD210277b	1.230	1.100	439.06	0.472	0.920	0.190	-0.208	0.063	0.682
70Virb	7.440	0.480	115.45	0.400	1.100	-0.030	-1.246	-0.716	0.545
HD37605b	2.300	0.250	50.98	0.677	0.800	0.390	-0.435	0.346	2.048
HD168443b [‡]	7.480	0.290	58.00	0.530	0.960	0.100	-1.332	-0.679	1.357
GJ3021b [†]	3.320	0.490	131.83	0.505	0.900	0.200	-0.383	-0.125	1.185
HD154857b	1.800	1.110	394.62	0.510	1.170	-0.230	-0.945	-0.874	-0.506
HD81040b	6.860	1.940	1003.92	0.526	0.960	-0.160	-2.103	-1.695	0.216
<i>Cluster C5</i>									
HD160691b [‡]	1.670	1.500	645.23	0.310	1.080	0.280	-0.248	0.915	0.205
HD202206c [‡]	2.440	2.550	1385.58	0.267	1.150	0.370	-0.951	1.403	-0.085
HD11977b	6.540	1.930	707.49	0.400	1.910	-0.210	-3.337	1.104	-1.800
UpsAndd ^{†,‡}	3.950	2.510	1272.09	0.242	1.300	0.130	-1.444	0.808	-0.739
HD196050b [†]	3.000	2.500	1374.86	0.280	1.100	0.000	-1.017	-0.251	-0.671
HD40979b [†]	3.320	0.811	256.33	0.230	1.080	0.194	0.054	0.488	0.258
HD187085b	0.750	2.050	970.36	0.470	1.220	0.050	-1.174	0.450	-0.491
HD33283b	0.330	0.168	22.58	0.480	1.240	0.366	-0.116	1.839	0.725
HD108147b	0.400	0.104	10.87	0.498	1.270	0.200	-0.223	1.270	0.390

TABLE 2—*Continued*

Planet	M_p	a	P	e	M_s	[Fe/H]	pc_1	pc_2	pc_3
HD169830c [‡]	4.040	3.600	2105.72	0.330	1.400	0.210	-2.532	1.360	-0.941
HD177830b	1.280	1.000	337.51	0.430	1.170	0.000	-0.489	0.101	-0.185
HD82943c [‡]	2.010	0.746	219.28	0.359	1.150	0.270	-0.204	1.069	0.428
HD216437b	2.100	2.700	1565.15	0.340	1.070	0.000	-1.091	-0.295	-0.657
HD12661c [‡]	1.570	2.560	1445.35	0.200	1.070	0.293	-0.407	0.948	-0.306
HD89307b	2.730	4.150	2737.38	0.270	1.270	-0.230	-2.148	-0.653	-2.027
HD73526b [‡]	2.900	0.660	193.66	0.190	1.020	0.280	0.474	0.694	0.481
HD117207b	2.060	3.780	2629.78	0.160	1.040	0.270	-0.981	0.702	-0.730
HD142b [†]	1.000	0.980	337.72	0.380	1.100	0.040	-0.119	0.083	-0.089
HD50499b	1.710	3.860	2456.46	0.230	1.270	0.230	-1.613	1.257	-1.146
HD169830b [‡]	2.880	0.810	224.83	0.310	1.400	0.210	-0.711	1.546	-0.164
HD216435b	1.490	2.700	1448.61	0.340	1.250	0.150	-1.283	0.898	-0.717
HD19994b [†]	2.000	1.300	465.64	0.200	1.350	0.230	-0.327	1.566	-0.472
HD82943b [‡]	1.750	1.190	441.84	0.219	1.150	0.270	0.087	1.124	0.008
HD38529b ^{†,‡}	0.780	0.129	14.35	0.290	1.390	0.313	0.185	2.120	0.066
HR810b	1.940	0.910	300.71	0.240	1.110	0.250	0.199	0.908	0.183
HD108874c [‡]	1.018	2.680	1601.77	0.250	1.000	0.140	-0.412	0.158	-0.498
UpsAndc ^{†,‡}	1.980	0.830	242.07	0.254	1.300	0.130	-0.168	1.017	-0.342
HD118203b ^h	2.130	0.070	6.09	0.309	1.230	0.100	0.151	0.676	0.081
47Umac [‡]	1.340	7.730	7730.20	-0.000	1.030	0.060	-2.425	-0.157	-2.795
HD62509b	2.900	1.690	587.98	0.020	1.860	0.190	-1.041	2.954	-1.817
HD72659b	2.960	4.160	3174.99	0.200	0.950	-0.140	-1.372	-1.282	-1.390

[†]Planets in multiple star systems.

[‡]Planets in multiple planetary systems.

^hHot Jupiters.

^{v^h}Very hot Jupiters.

^tTransiting planets.